Chemical and Isotopic Analytical Procedures

Prior to sample digestion, the powder sample splits were leached with 6N-HCl at 80ºC for two hours, rinsed with de-ionized water, and then dried. The samples were weighed and digested with HF and $HClO_4$, and then dissolved in HCl.

Part of aliquot was taken from the solution by a micro-pipette and served for trace element analysis with dilution by nitric acid. Concentrations of rare earth and 17 other trace elements (Sc, Co, Ni, Cu, Rb, Sr, Y, Zr, Nb, Cs, Ba, Hf, Ta, Tl, Pb, Th, and U) were analyzed using by inductively coupled plasma mass spectrometry (ICP-MS) using an Agilent 7500ce system fitted with PFA sample introducing and a Pt-inject torch system. The ICP-MS system was operated in no collision gas and multi-tune acquisition mode. This combination allowed a wide range of elements to be precisely determined using pulse counting detection with the hydrofluoric acid containing sample solution being delivered directly into the plasma. Sample dissolution, preparation and measurement were described by Chang et al. [2003] and Nakamura & Chang [2007]. Analytical accuracy and precision for ICP-MS analyses, estimated from repeated measurements of international reference rocks (JB-1a of GSJ, BCR-2 and BIR-1 of USGS) were mostly better than 5% and 3%, respectively.

Hf was separated by a single-column method using Ln-Spec resin (Eichrom Technologies, Inc.®) following *Münker et al.* [2001]. The total procedural blank for Hf was less than 25pg. Hf isotope ratios were measured on a sector-type multi-collector ICP-MS (Neptune®; Thermo Fischer Scientific) at IFREE, JAMSTEC. Mass fractionation factor was determined by the $^{179}Hf/^{177}Hf$ ratio and isotope ratios were normalized to a $^{179}Hf/^{177}Hf$ value of 0.7325 using an exponential law. ^{173}Yb and ^{175}Lu peaks were monitored to correct for interference of ^{176}Yb and ^{176}Lu on the ^{176}Hf peak. Repeated measurement of the standard JMC475 provided $^{176}Hf/^{177}Hf$ ratios of 0.282141 ± 0.000007 (2σ, n=8) during the measurements. The reported $^{176}Hf/^{177}Hf$ ratio is adjusted by referring a JMC475 value of 0.28216. Analytical uncertainties shown in the table are in 2σ level.

Nd was separated from the first eluent of the Hf column and further separated by cation exchange resin (AG50W-X8) by HCl for REEs and the second separation for Nd by a miniature cation exchange resin (AG50W-X8) column using HIBA (Hirahara et al., in press). The collected Nd fractions were dissolved in 1 M HNO3. Approximately 100 - 50 ng of each Nd sample was loaded onto an out-gassed Re-filament and dried at 0.6 A. The filament was slowly heated and kept at 2.0 A for 1 min. $^{143}Nd/^{144}Nd$ ratios were measured using TIMS (TRITON TI®, Thermo Fisher Scientific) equipped with nine Faraday cups at IFREE, JAMSTEC. Standard JNd-1 was analyzed during analyses and $^{143}Nd/^{144}Nd$ = 0.512096 ± 0.000009 (2σ, n=4).

Epsilon values were calculated relative to the following values for the Bulk Earth: $^{176}Hf/^{177}Hf$ = 0.282772; $^{143}Nd/^{144}Nd$ = 0.512638

REFERENCES

Chang, Q., Shibata, T., Shinotsuka, K., Yoshikawa, M. & Tatsumi, Y. (2003).Precise determination of trace elements in geological standard rocks using inductively coupled plasma mass spectrometry (ICP-MS). Frontier Research on Earth Evolution 1, 357-362.

Hirahara, Y., Takahashi, T., Miyazaki, T., Vaglarov, B. S., Chang, Q., Kimura, J.-I., Tatsumi, Y. (2009). Precise Nd isotope analysis of igneous rocks using cation exchange chromatography and thermal ionization mass spectrometry (TIMS), JAMSTEC Report R&D, S. I., 65-72

Münker, C., Weyer, S., Scherer, E., Mezger, K. (2001). Separation of high field strength elements (Nb, Ta, Zr, Hf) and Lu from rock samples for MC-ICPMS measurements. G-cubed 2, paper number 2001GC000183

Nakamura, K. & Chang, Q. (2007). Precise determination of ultralow (sub-ng g-1) level rare earth elements in ultramafic rocks by quadrupole ICP-MS. Geostandards and Geoanalytical Research 31, 185-197.

$^{40}Ar/^{39}Ar$ Geochronology Results From Mafic Igneous Clasts in southern Louisiana Salt Domes

By

Matt Heizler

OCT. 19, 2009

Prepared for

Robert J. Stern
Geosciences Department
University of Texas at Dallas
800 W. Campbell Road
Richardson TX 75080-3021 U.S.A.

NEW MEXICO GEOCHRONOLOGICAL RESEARCH LABORATORY (NMGRL)

CO-DIRECTORS

DR. MATTHEW T. HEIZLER

DR. WILLIAM C. MCINTOSH

LABORATORY TECHNICIAN

LISA PETERS

Internal Report # : NMGRL-IR-617

Introduction

Dr. Robert Stern from UT-Dallas submitted two mineral samples for $^{40}Ar/^{39}Ar$ dating. Hornblende and biotite were recovered from mafic igneous clasts within the southern Louisiana salt domes and provide well-constrained $^{40}Ar/^{39}Ar$ results.

$^{40}Ar/^{39}Ar$ Analytical Methods and Results

The samples were irradiated in two separate irradiations at the UGGS TRIGA reactor in Denver, CO along with the standard Fish Canyon tuff sanidine as a neutron flux monitor. Both Weeks Island hornblende and W26 biotite were heated using the incremental step-heating method within a double vacuum Mo furnace and the flux monitor crystals were fused using a CO_2 laser. Additional methodology specific to this report is summarized in Table 1 and general operational details for the NMGRL can be found at internet site http://geoinfo.nmt.edu/publications/openfile/argon/home/html.

Age spectra diagrams are given in Figures (1a, 1b) and complete analytical data are provided in Table 2. The Weeks Island hornblende has an overall saddle shaped spectrum with the majority of the ^{39}Ar released defining a flat segment with a plateau age of 160.1±0.7 Ma (Fig. 1a; Tables 1, 2). The initial part of the spectrum has many small steps with high uncertainty due to the fact that the sample did not begin to degas significantly until reaching incremental steps greater than about 1100°C. The final step is significantly older than the plateau steps and the integrated age is 167.1±0.8 Ma. Isochron analysis for Weeks Island hornblende shows a linear array (MSWD = 2.2) for steps L-Q and an apparent age of 159.2±0.7 Ma.

W26 biotite has an overall flat spectrum with the final ~84% of the ^{39}Ar released defining a plateau age of 158.6±0.2 Ma (Fig. 1b; Tables 1, 2). Steps D and F have relatively high analytical error due to mass spectrometer electronic instabilities occurring during these steps. Isochron analysis is not useful for this sample due to data clustering related to constant and high $^{40}Ar^*$ yields.

Discussion

Overall the data are well behaved and thus the interpretation for these samples is straightforward. Although the Weeks Island hornblende plateau and isochron ages agree at the 1 sigma level we prefer the isochron age of 159.2±0.7 Ma because excess ^{40}Ar is indicated by the trapped initial $^{40}Ar/^{36}Ar$ value of 351±13 (Fig. 2). This hornblende age represents the time at which the sample cooled below ca. 500°C (the nominal closure temperature for argon in hornblende). The W26 biotite age of 158.6±0.2 Ma records cooling below the biotite closure temperature of about 300°C.

If these rocks underwent rapid cooling, the apparent argon ages could represent the crystallization ages of the mafic rock fragments thereby placing a maximum age on the salt domes.

References cited

Renne, P.R., Swisher, C.C., Deino, A.L., Karner, D.B., Owens, T.L., and DePaolo, D.J., 1998. Intercalibration of standards, absolute ages and uncertainties in $^{40}Ar/^{39}Ar$ dating. Chemical Geology, 145, 117-152.

Steiger, R.H., and Jäger, E., 1977. Subcommission on geochronology: Convention on the use of decay constants in geo- and cosmochronology. Earth and Planet. Sci. Lett., 36, 359-362.

Taylor, J.R., 1982. An Introduction to Error Analysis: The Study of Uncertainties in Physical Measurements,. Univ. Sci. Books, Mill Valley, Calif., 270 p.

York, D., 1969. Least Squares fitting of a straight line with correlated errors. Earth. Planet. Sci. Lett., 5, 320-324.

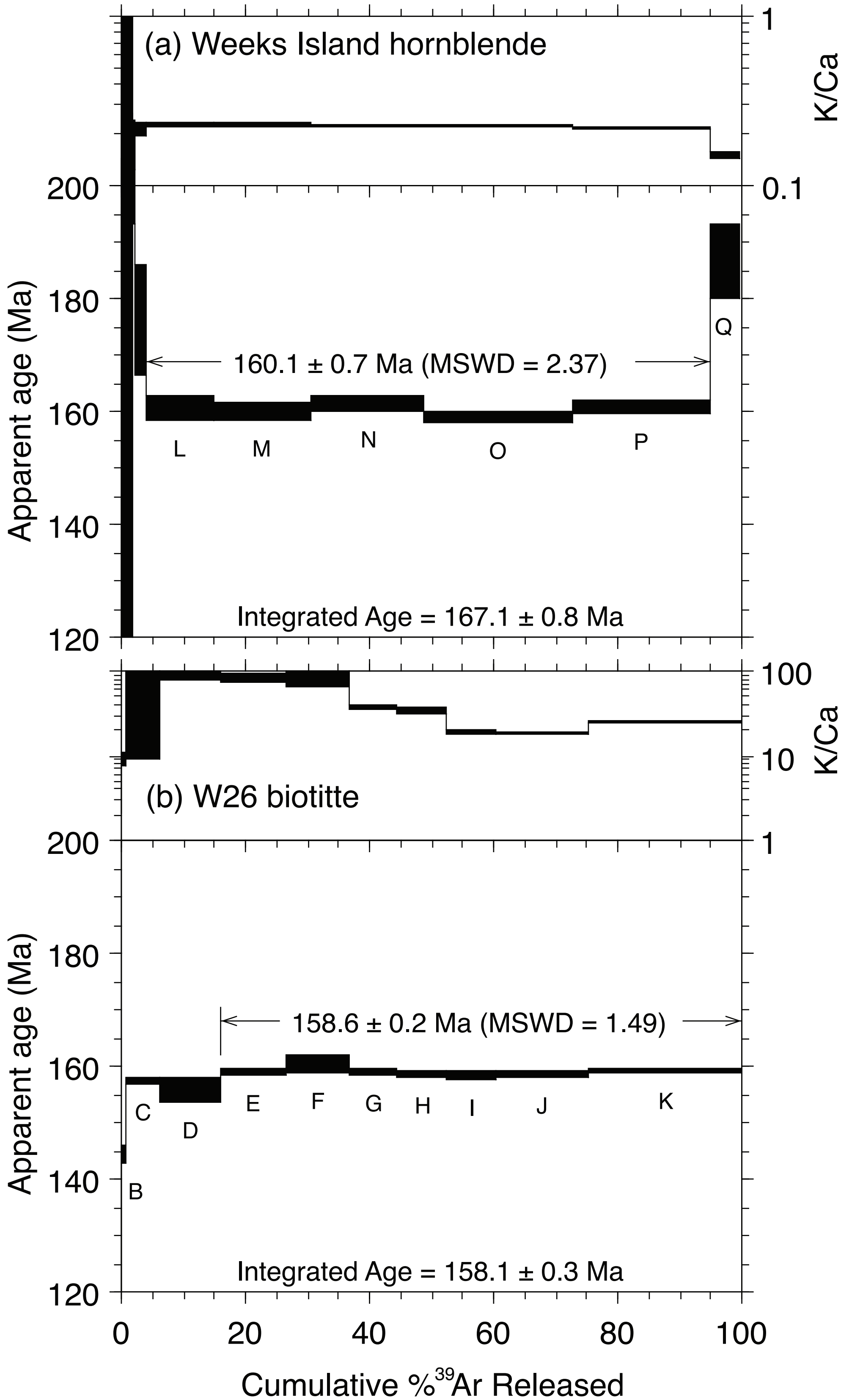

Figure 1. Age and K/Ca spectra for Weeks Island hornblende (a) and W26 biotite (b).

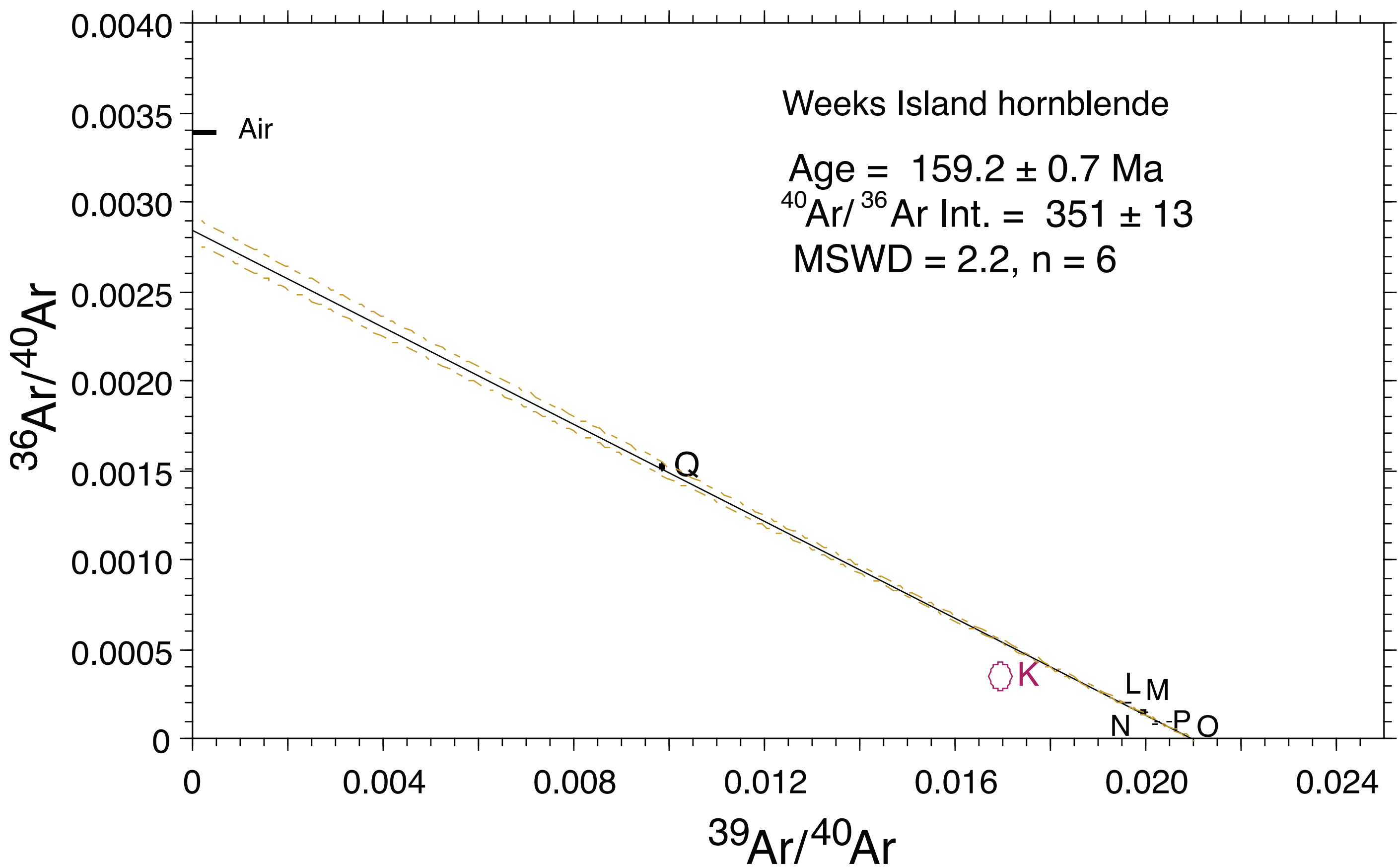

Figure 2 Isochron diagram for Weeks Island hornblende. The very low precision steps A-J are omitted for diagram clarity and step K is shown but omitted from the York (1969) regression.

Table 1. Summary of age information and analytical methods.

Summary

Sample	L#	Irrad	Min	Weight (mg)	analysis	n	%^{39}Ar	MSWD	Age	±1σ
Weeks Island	58026-01	NM-220B	H	11.05	Plateau	5	90.7	2.4	160.1	0.7
					Isochron	6	95.7	2.2	159.2	0.7
W26	58931-01	NM-223K	B	6.97	Plateau	7	83.9	1.5	158.6	0.2

L# = Lab number
Irrad = Irradiation number
Min = mineral: H=Hornblende. B=Biotite
n = number of steps for plateau isochron age
%^{39}Ar = percentage of total ^{39}Ar comprising the plateau or isochron steps.

Methods

Sample preparation and irradiation:
Mineral separates provided by Bob Stern and further purified by hand-picking by NMGRL.
Separates were loaded into machined Al discs and irradiated for 60 hours, USGS TRIGA Reactor, Denver
Neutron flux monitor Fish Canyon Tuff sanidine (FC-2). Assigned age = 28.02 Ma (Renne et al., 1998)
_

Instrumentation:
Mass Analyzer Products 215-50 mass spectrometer on line with automated all-metal extraction system.
Samples step-heated in Mo double vacuum resistance furnace.
Furnace analysis: Reactive gases removed during a 5 minute (hornblende) or 6 minute (biotitie(heating with a SAES GP-50 getter operated at ~450°C.
Additional cleanup (3-5 minutes) following heating with 2 SAES GP-50 getters, 1 operated at ~450°C and 1 at 20°C.
Gas also exposed to cold finger -140°C during heating.

Analytical parameters:
Electron multiplier sensitivity about 1.0×10^{-16} moles/pA
Total system blank and background: 175, 1.2, 0.5, 1.9, 0.6 x 10^{-17} moles for masses 40, 39, 38, 37, 36, respectively.
J-factors determined to a precision of ~± 0.1% by CO_2 laser-fusion of 6 single crystals from each of 4 radial positions around the irradiation tray.
Correction factors for interfering nuclear reactions were determined using K-glass and CaF_2 and are as follows:
$(^{40}Ar/^{39}Ar)_K = 0.010 \pm 0.002$; $(^{36}Ar/^{37}Ar)_{Ca} = 0.00028 \pm 0.00002$; and $(^{39}Ar/^{37}Ar)_{Ca} = 0.00070 \pm 0.00005$.

Table 2. Argon isotopic results.

	ID	Temp (°C)	$^{40}Ar/^{39}Ar$	$^{37}Ar/^{39}Ar$	$^{36}Ar/^{39}Ar$ (x 10^{-3})	$^{39}Ar_K$ (x 10^{-15} mol)	K/Ca	$^{40}Ar^*$ (%)	^{39}Ar (%)	Age (Ma)	±1σ (Ma)
	Weeks Island Hornblende, 11.05 mg, J=0.0019344±0.30%, D=1.0014±0.001, NM-220B, Lab#=58026-01										
x	A	900	952.7	4.213	2810.0	0.070	0.12	13.5	0.7	402	30
x	B	950	249.7	1.044	393.6	0.017	0.49	53.6	0.9	415	60
x	C	1000	238.9	3.574	428.6	0.017	0.14	47.2	1.1	357	49
x	D	1050	186.1	2.969	201.9	0.024	0.17	68.1	1.3	396	39
x	E	1080	122.6	0.9098	74.43	0.029	0.56	82.1	1.6	321	29
x	F	1090	143.3	2.220	34.27	0.016	0.23	93.1	1.8	415	54
x	G	1100	132.6	3.268	128.2	0.016	0.16	71.7	2.0	305	53
x	H	1110	99.21	3.400	-26.2296	0.023	0.15	108.1	2.2	341	37
x	I	1120	37.13	-4.3000	92.61	-0.005	-	25.4	2.1	32	130
x	J	1120	79.18	2.854	27.54	0.038	0.18	90.0	2.5	233	20
x	K	1130	58.82	2.388	20.81	0.173	0.21	89.9	4.3	175.9	4.9
	L	1140	50.85	2.279	10.24	1.04	0.22	94.4	15.1	160.4	1.0
	M	1150	49.94	2.268	7.828	1.52	0.23	95.7	30.9	159.81	0.73
	N	1180	49.41	2.301	4.365	1.74	0.22	97.8	48.9	161.40	0.70
	O	1220	48.68	2.320	4.644	2.32	0.22	97.6	73.0	158.80	0.58
	P	1260	49.30	2.376	4.820	2.13	0.21	97.5	95.0	160.64	0.60
x	Q	1650	101.3	3.431	153.5	0.479	0.15	55.5	100.0	186.5	3.4
	Integrated age ± 1σ			n=17		9.7	0.21	K2O=0.17%		166.97	0.73
	Plateau ± 1σ	steps L-P		n=5	MSWD=2.37	8.8			90.7	160.10	0.66
	W26, Biotite, 6.97 mg, J=0.0024166±0.10%, D=1.004±0.001, NM-223K, Lab#=58931-01										
x	A	650	108.9	0.2732	290.3	1.15	1.9	21.2	0.3	97.9	3.8
x	B	750	42.56	0.0572	27.51	2.39	8.9	80.9	1.1	144.16	0.82
x	C	850	40.32	-0.0820	9.038	17.6	-	93.4	6.3	157.04	0.31
x	D	920	40.32	0.0060	10.35	32.9	85.2	92.4	16.1	155.5	1.1
	E	1000	41.47	0.0062	11.42	35.3	82.4	91.9	26.7	158.86	0.32
	F	1075	39.87	0.0311	4.986	33.9	16.4	96.3	36.8	160.06	0.81
	G	1110	39.31	0.0140	4.243	26.3	36.5	96.8	44.7	158.68	0.27
	H	1180	40.13	0.0149	7.390	26.3	34.1	94.6	52.6	158.24	0.31
	I	1210	40.07	0.0278	7.276	26.6	18.3	94.6	60.6	158.16	0.32
	J	1250	39.43	0.0280	4.826	49.2	18.2	96.4	75.3	158.48	0.26
	K	1300	38.93	0.0206	2.796	82.7	24.8	97.9	100.0	158.88	0.23
	Integrated age ± 1σ			n=11		334.3	33.7	K2O=7.62%		158.07	0.28
	Plateau ± 1σ	steps E-K		n=7	MSWD=1.49	280.3			83.9	158.62	0.20

Notes:

Isotopic ratios corrected for blank, radioactive decay, and mass discrimination, not corrected for interfering reactions.
Errors quoted for individual analyses include analytical error only, without interfering reaction or J uncertainties.
Integrated age calculated by summing isotopic measurements of all steps.
Integrated age error calculated by quadratically combining errors of isotopic measurements of all steps.
Plateau age is inverse-variance-weighted mean of selected steps.
Plateau age error is inverse-variance-weighted mean error (Taylor, 1982) times root MSWD where MSWD>1.
Plateau error is weighted error of Taylor (1982).
Decay constants and isotopic abundances after Steiger and Jäger (1977).
x symbol preceding sample ID denotes analyses excluded from plateau age calculations.
Weight percent K_2O calculated from ^{39}Ar signal, sample weight, and instrument sensitivity.
Ages calculated relative to FC-2 Fish Canyon Tuff sanidine interlaboratory standard at 28.02 Ma
Decay Constant (LambdaK (total)) = 5.543e-10/a
Correction factors:

$(^{39}Ar/^{37}Ar)_{Ca}$ = 0.0007 ± 5e-05
$(^{36}Ar/^{37}Ar)_{Ca}$ = 0.00028 ± 2e-05
$(^{38}Ar/^{39}Ar)_K$ = 0.013
$(^{40}Ar/^{39}Ar)_K$ = 0.01 ± 0.002

Descriptions of Electron Backscattered Images (DR Figures 1-9)

Figure DR1. Typical appearance of fresh clinopyroxene. Zoned clinopyroxene (W26) have core compositions with either high (1a) or low Si (1b) silica contents. Compositions of rims and matrix clinopyroxene are similar, indicating equilibrium between the melt and final crystallization of clinopyroxene.

Figure DR2. Clinopyroxene in the more altered samples (2EO and W25) is replaced by quartz. These clinopyroxene also have a thin reaction rim of titanite. 2a. Relict clinopyroxene in quartz with titanite rim (W25). 2b. Euhedral pseudomorph of quartz with titanite rim (2EO).

Figure DR3. Mg-Al spinel is found in all samples and, like clinopyroxene, commonly displays a thin alteration selvage of titanite. 3a. Homogenous grain of chromite (W26). 3b. Chromite intergrowth with clinopyroxene (W26).

Figure DR4. Amphibole phenocryst from 2EO. Alteration selvage and veins crosscutting the amphibole are vermiculite.

Figure DR5. Biotite is observed in all samples, as phenocrysts, overgrowths on quartz, and microcrysts in matrix. 5a. Biotite intergrowth with jacobsitic magnetite and quartz. 5b. Quartz in association with biotite and vermiculite.

Figure DR6. Titanite is found in all samples as euhedral crystals (e.g images from W25), as subhedral to anhedral microcrysts distributed throughout a vermiculite matrix, and as overgrowths on vermiculite, clinopyroxene, and quartz crystals (Fig. 2, 3).

Figure DR7. 7a. Pyrite can occur as either anhedral co-existing with clinopyroxene, titanite, and vermiculite in the matrix or as euhedral grains within a vermiculite vein.

Figure DR8. Alteration phenomena in 2EO. 8a. Mcgillite co-exists with calcite at the edge of vermiculite. 8b. Hematite occurs along fractures within vermiculite, indicating late-stage precipitation.

Figure DR9. Alteration products in W26. 9a. Vermiculite with titanite rim. 9b, 9c. Orthoclase is typically associated with quartz, vermiculite and chlorite.

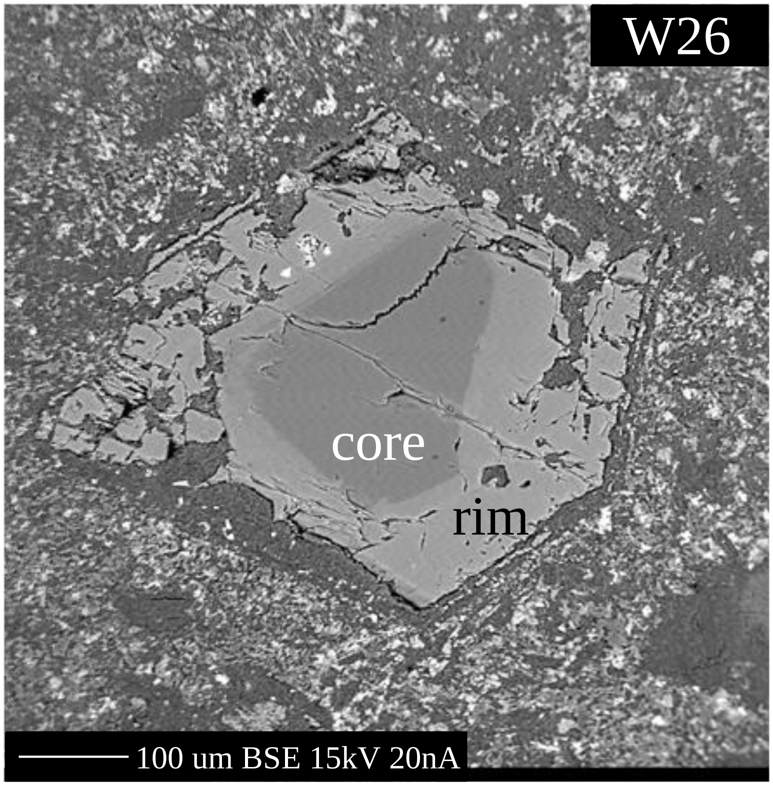

Figure DR1a

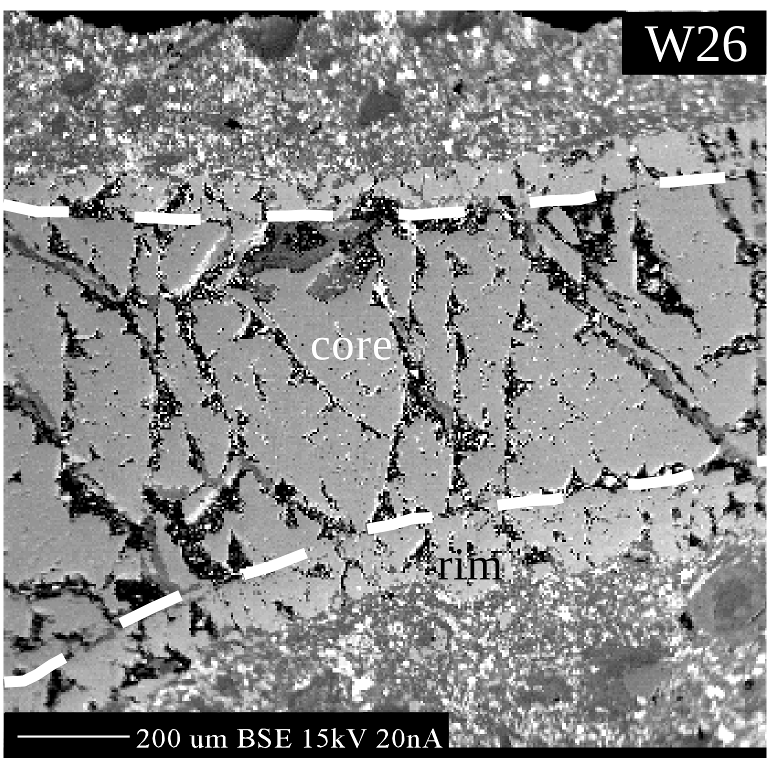

Figure DR1b

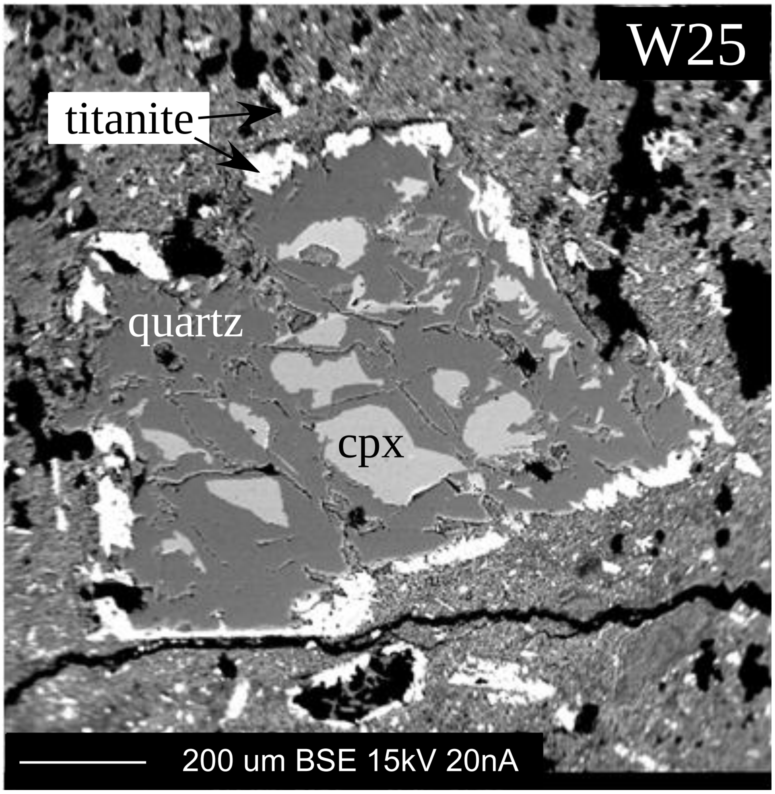

Figure DR2a

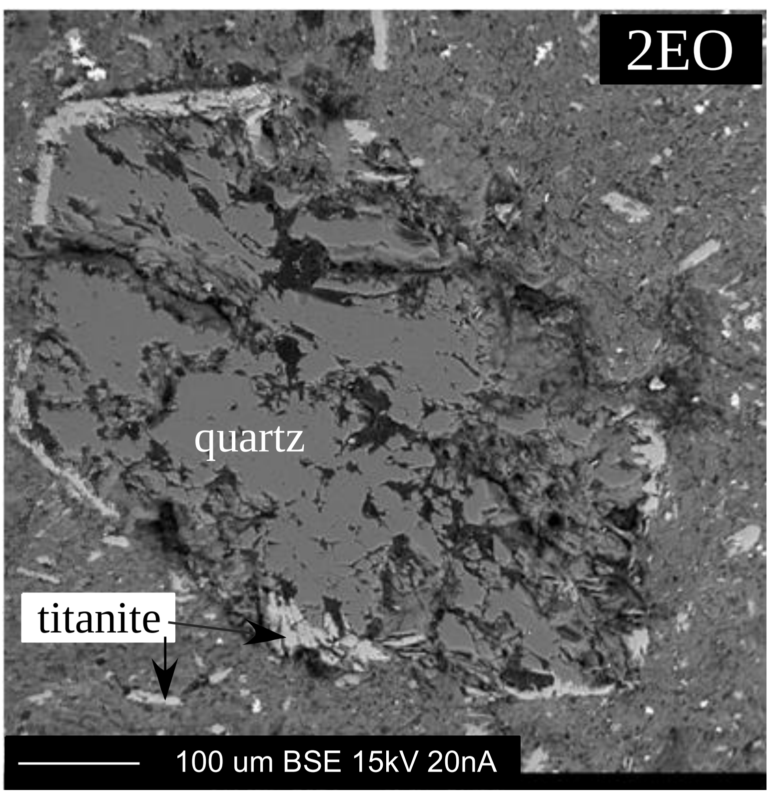

Figure DR2b

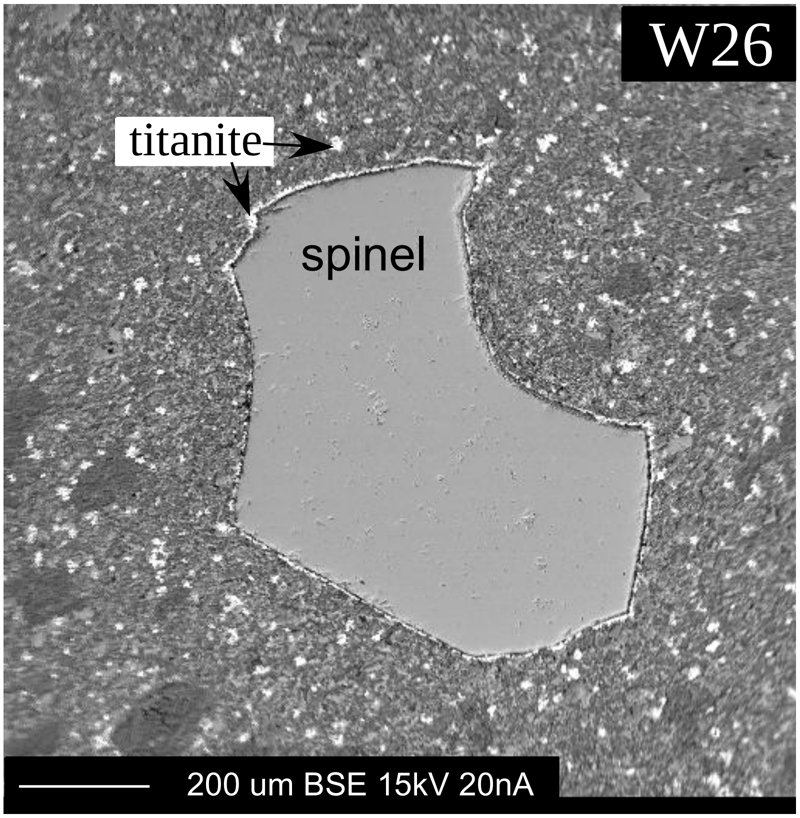

Figure DR3a

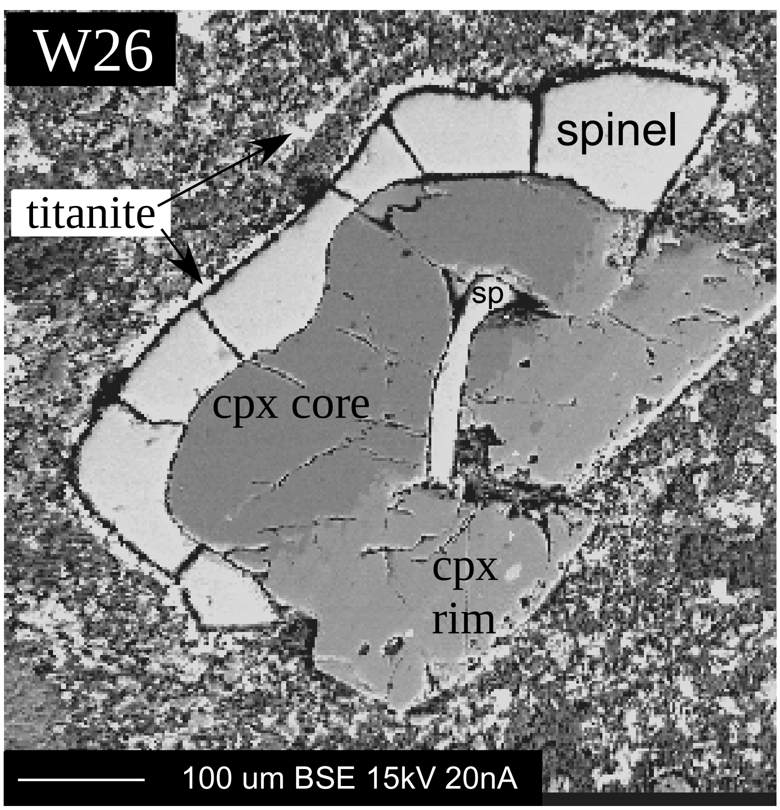

Figure DR3b

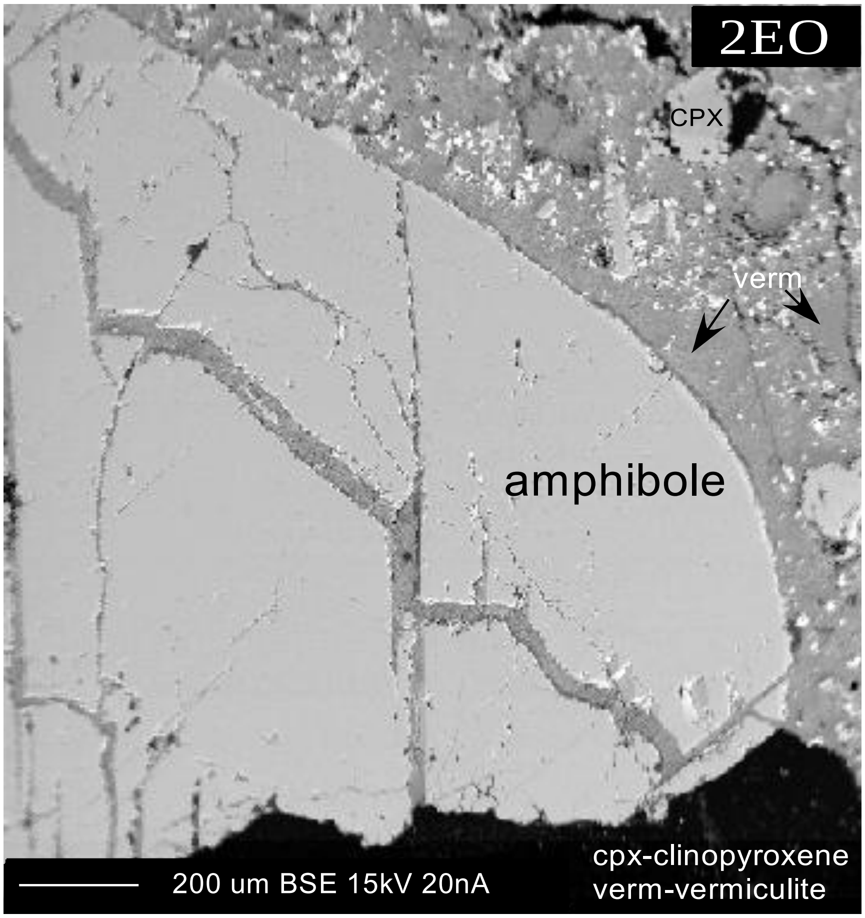
2EO
CPX
verm
amphibole
200 um BSE 15kV 20nA
cpx-clinopyroxene
verm-vermiculite

Figure DR4

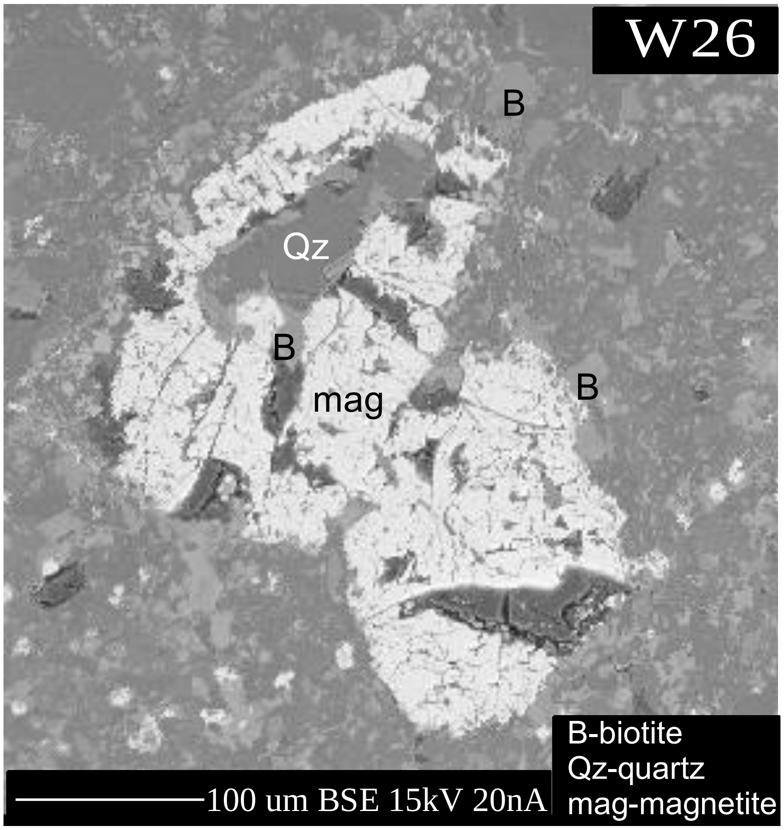

Figure DR5a

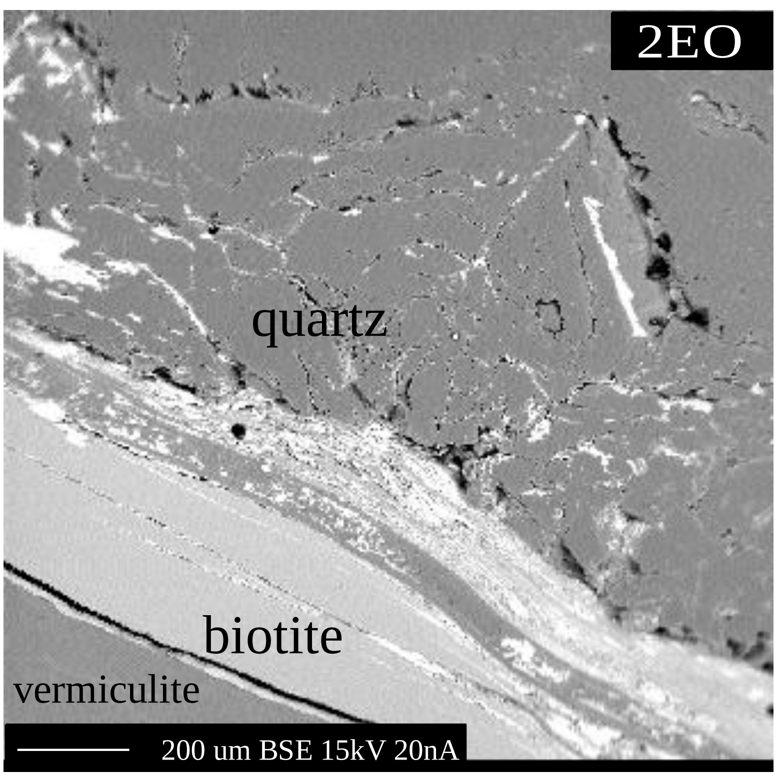

Figure DR5b

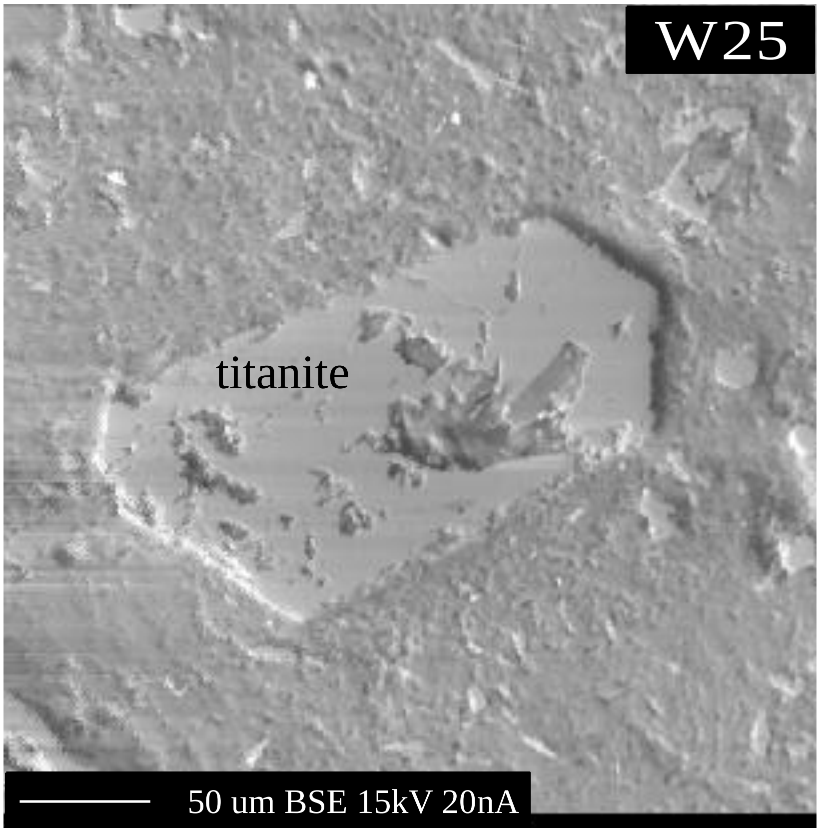

Figure DR6

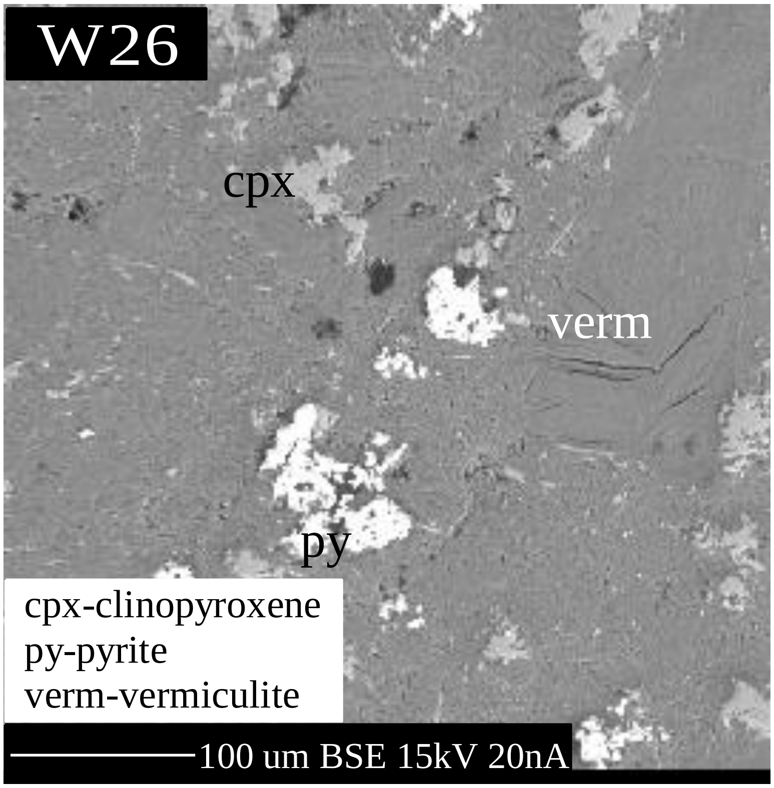

Figure DR7a

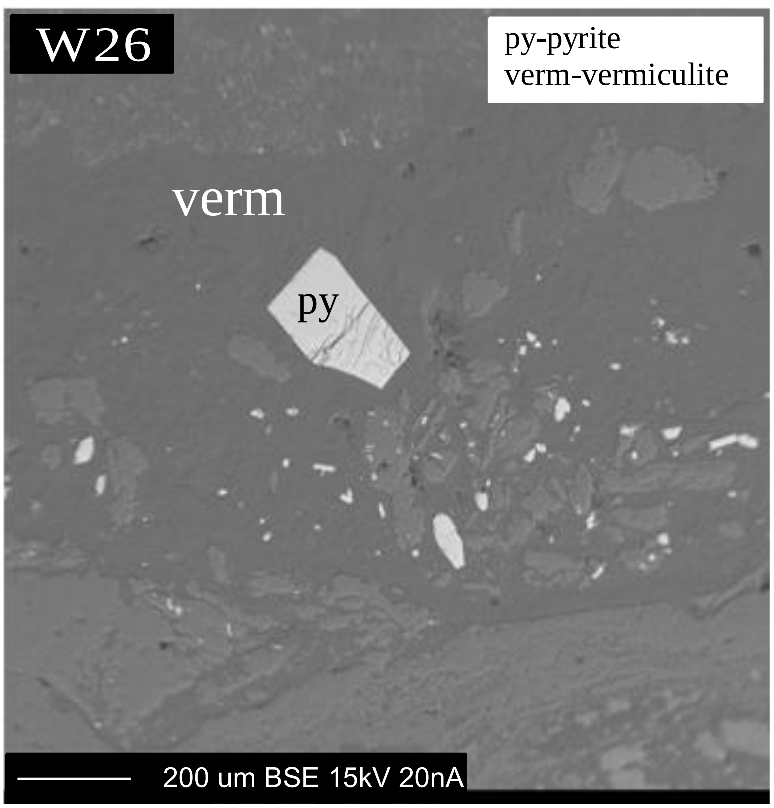

Figure DR7b

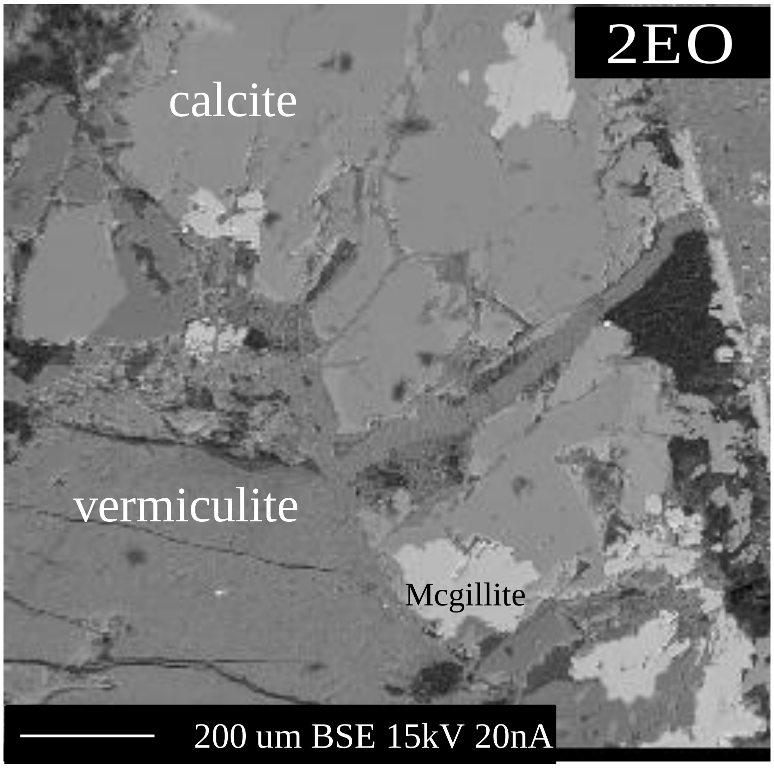

Figure DR8a

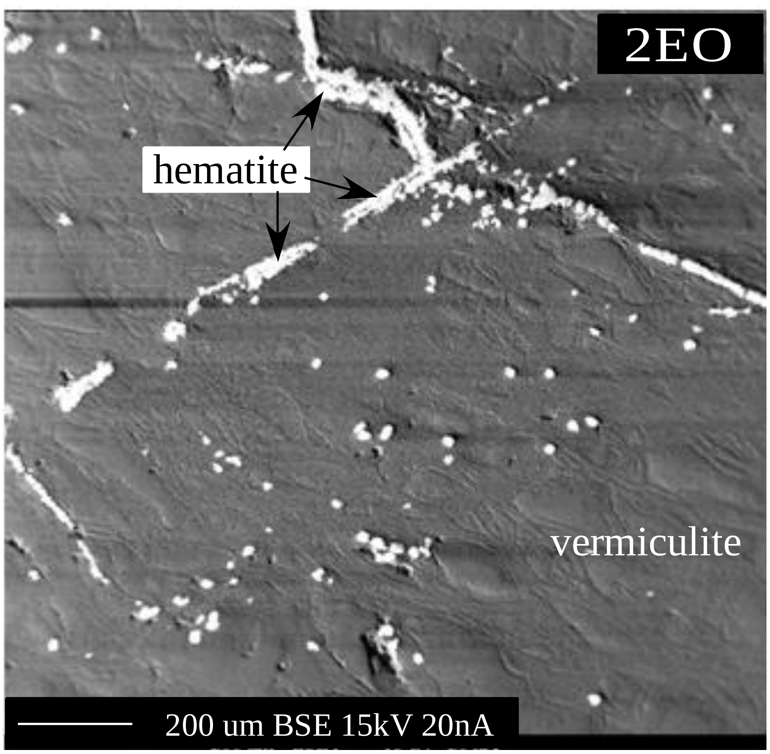

Figure DR8b

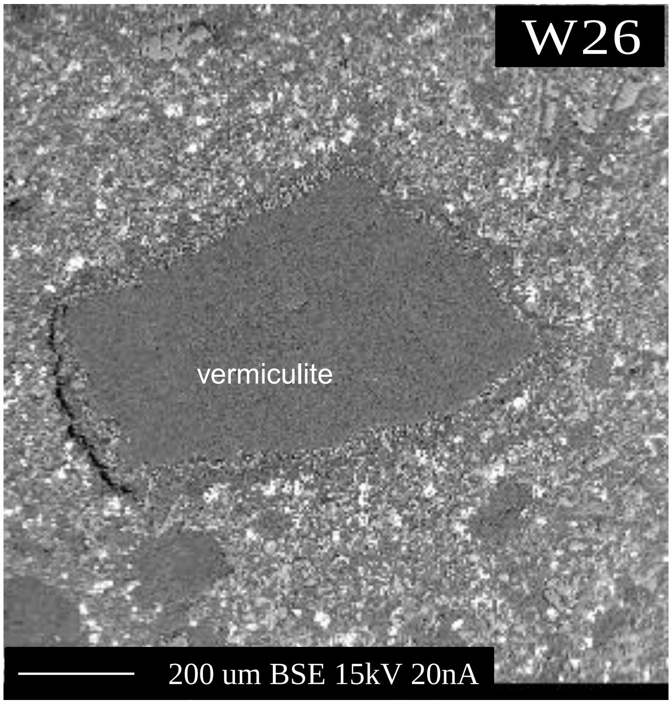

Figure DR9a

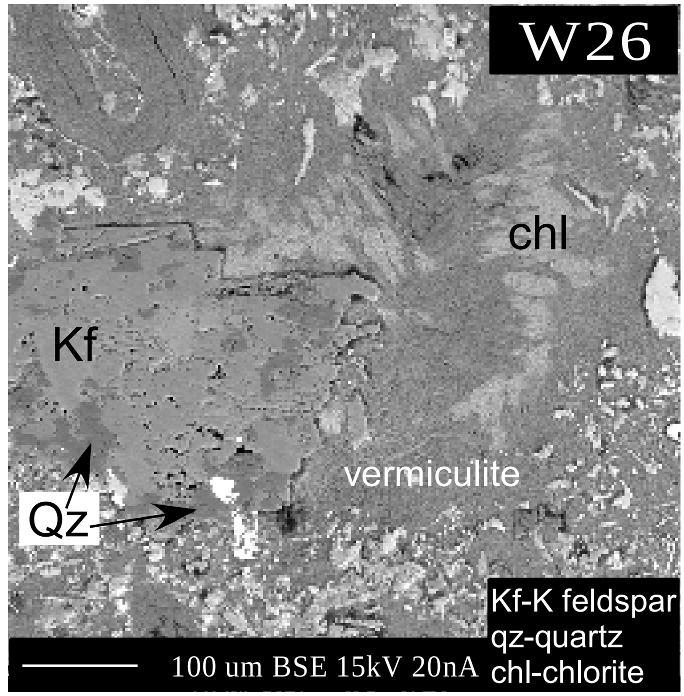

9b

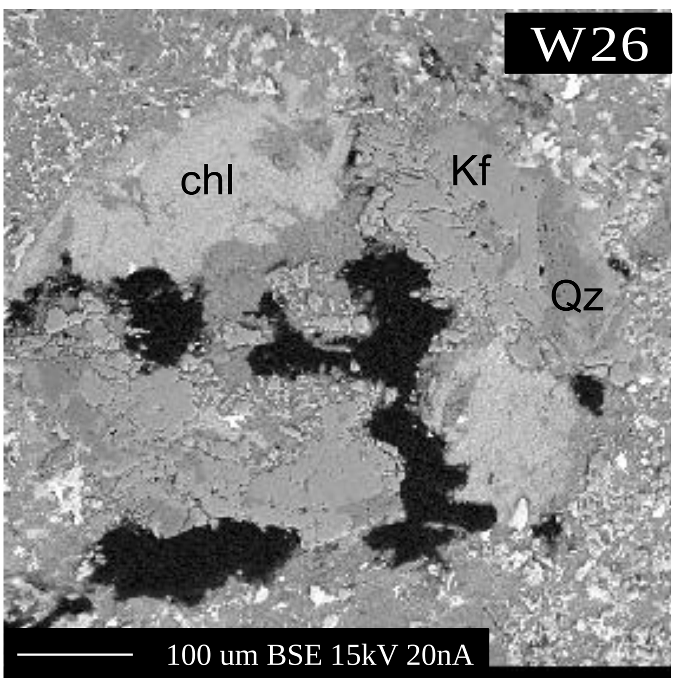

Figure DR9c

Table DR1.

Analyte Symbc	SiO2 %	Al2O3%	Fe2O3(T)%	MnO%	MgO%
Detection Limi	0.01	0.01	0.01	0.001	0.01
Analysis Methc	FUS-ICP	FUS-ICP	FUS-ICP	FUS-ICP	FUS-ICP
2E-O	33.21	10.13	11.32	0.986	21.74
W26	34.76	11.88	11.99	0.918	14.68
25-W	31.4	11.19	10.68	1.015	20.54

sample	ICP-MS data	Sc	Co	Ni	Cu
2-EO	µg g-1	36.6	70.1	46.2	18.6
	1sd	0.2	0.2	0.4	0.2
	rsd,%	0.4	0.3	0.9	1.0
W-26	µg g-1	29.7	46.9	31.0	15.9
	1sd	0.1	0.4	0.3	0.2
	rsd,%	0.2	0.9	0.8	1.2
W-25	µg g-1	46.1	5.30	30.6	10.8
	1sd	0.6	0.07	0.5	0.3
	rsd,%	1.2	1.3	1.7	2.6
W-25	µg g-1	45.7	5.28	29.8	10.7
(repeated)	1sd	0.6	0.06	0.4	0.4
	rsd,%	1.3	1.1	1.2	3.6
Reference rock:					
BHVO-2G	µg g-1	29.8	43.4	116	128
	1sd	0.4	0.4	2	0.7
	rsd,%	1.3	0.8	1.4	0.6

sample	ICP-MS data	Eu	Gd	Tb	Dy
2-EO	µg g-1	3.16	8.74	1.28	6.61
	1sd	0.03	0.03	0.01	0.05
	rsd,%	0.8	0.3	0.6	0.8
W-26	µg g-1	3.56	10.1	1.52	8.05
	1sd	0.04	0.0	0.01	0.05
	rsd,%	1.0	0.5	0.6	0.7
W-25	µg g-1	3.57	10.8	1.67	9.21
	1sd	0.01	0.1	0.02	0.10
	rsd,%	0.3	1.0	1.0	1.1
W-25	µg g-1	3.51	10.7	1.69	9.35
(repeated)	1sd	0.03	0.1	0.02	0.09
	rsd,%	1.0	0.8	1.0	0.9
Reference rock:					
BHVO-2G	µg g-1	2.06	6.34	0.960	5.33
	1sd	0.02	0.06	0.013	0.04
	rsd,%	1.2	1.0	1.4	0.7

Table DR1.

DR Table 1: Chemical Analyses

CaO%	Na2O%	K2O%	TiO2%	P2O5%	s on Ignition %
0.01	0.01	0.01	0.001	0.01	
FUS-ICP	FUS-ICP	FUS-ICP	FUS-ICP	FUS-ICP	FUS-ICP
4.44	1.03	0.24	2.844	0.73	12.19
6.08	0.32	2.47	4.029	1.05	9.02
5.12	0.26	0.49	3.588	0.68	14

Rb	Sr	Y	Zr	Nb	Cs
2.75	121	25.9	547	155	0.354
0.05	0	0.1	4	1	0.003
2.0	0.3	0.4	0.8	0.8	0.9
119	449	32.3	729	211	0.267
0.7	4	0.2	4	1	0.002
0.6	0.9	0.7	0.5	0.4	0.9
18.8	11.5	38.4	823	242	b.d.
0.1	0.1	0.2	3	2	
0.5	1.0	0.5	0.4	0.8	
18.5	11.1	39.2	823	233	b.d.
0.2	0.1	0.5	6	1	
1.0	1.2	1.4	0.8	0.4	
8.81	389	23.5	171	17.0	0.090
0.07	2	0.1	1	0.1	0.003
0.8	0.4	0.5	0.6	0.5	3.2

Ho	Er	Tm	Yb	Lu	Hf
1.14	2.90	0.370	2.30	0.325	13.10
0.01	0.03	0.003	0.02	0.005	0.14
0.9	0.9	0.9	1.1	1.5	1.0
1.44	3.76	0.491	3.07	0.443	16.63
0.01	0.03	0.004	0.02	0.005	0.11
0.9	0.9	0.9	0.7	1.1	0.7
1.65	4.27	0.544	3.35	0.468	18.8
0.02	0.02	0.010	0.03	0.007	0.1
1.0	0.4	1.9	1.0	1.4	0.5
1.70	4.35	0.559	3.41	0.476	18.7
0.01	0.06	0.010	0.04	0.009	0.1
0.8	1.4	1.8	1.2	2.0	0.5
0.989	2.60	0.336	2.01	0.278	4.60
0.012	0.03	0.004	0.04	0.005	0.03
1.3	1.2	1.1	1.8	1.7	0.8

Table DR1.

Total%	Be ppm	V ppm
0.01	1	5
FUS-ICP	FUS-ICP	FUS-ICP
98.87	2	208
97.21	3	289
98.97	2	230

Ba	La	Ce	Pr	Nd	Sm
71.7	21.5	61.4	8.91	40.2	9.87
0.6	0.1	0.3	0.04	0.3	0.06
0.9	0.2	0.4	0.5	0.7	0.6
309	32.5	82.0	10.6	45.9	10.7
2	0.2	0.5	0.1	0.4	0.1
0.6	0.7	0.6	0.5	0.9	0.9
41.8	33.8	77.3	10.3	44.8	11.2
0.4	0.1	0.4	0.1	0.4	0.1
1.0	0.4	0.6	0.5	1.0	0.7
40.6	32.4	74.4	9.87	43.3	10.9
0.4	0.1	0.4	0.02	0.2	0.1
1.1	0.3	0.5	0.2	0.4	1.0
130	15.0	37.2	5.28	24.3	6.10
1	0.1	0.3	0.04	0.1	0.06
1.0	0.6	0.7	0.7	0.6	1.0

Ta	Tl	Pb	Th	U
9.33	0.028	1.96	7.07	2.25
0.09	0.002	0.02	0.07	0.03
1.0	5.8	1.1	1.0	1.3
12.94	0.064	3.73	6.19	3.24
0.07	0.001	0.02	0.03	0.01
0.6	1.6	0.6	0.5	0.3
14.5	b.d.	1.16	10.0	2.62
0.1		0.01	0.0	0.02
0.5		1.0	0.4	0.8
13.9	b.d.	1.08	10.3	2.59
0.0		0.02	0.0	0.01
0.1		2.2	0.4	0.5
1.13	0.014	1.50	1.23	0.425
0.00	0.001	0.01	0.01	0.005
0.2	6.2	1.0	0.7	1.2

Table DR2 . Representative mineral compositions

	Clinopyroxene						
	w26				2EO		
	lowSi-core	highSi-core	cpx-rim	mtx cpx	lowSi-core	highSi-core	cpx-rim
SiO_2	49.36	52.10	43.25	45.02	48.39	52.42	43.18
TiO_2	1.26	0.03	3.95	3.85	2.17	0.10	4.23
Al_2O_3	8.23	3.54	9.53	7.04	5.90	3.52	10.25
Cr_2O_3	0.24	1.12	0.08	0.03	0.28	1.23	0.02
FeO	5.39	2.90	7.03	7.16	5.70	2.61	7.09
MnO	0.10	0.02	0.12	0.17	0.09	0.12	0.14
MgO	14.96	18.11	12.10	13.02	14.47	17.73	11.52
CaO	19.55	20.82	22.23	23.51	22.76	21.08	22.91
Na_2O	0.95	0.46	0.54	0.50	0.51	0.68	0.61
Total	100.04	99.09	98.82	100.29	100.27	99.48	99.94
	Numbers of ions on the basis of 6 O						
Si	1.804	1.903	1.580	1.645	1.768	1.915	1.578
Al(IV)	0.196	0.097	0.410	0.303	0.232	0.085	0.422
Al(VI)	0.158	0.056	0.000	0.000	0.022	0.067	0.019
Fe(iii)	0.044	0.037	0.000	0.000	0.000	0.082	0.000
Cr	0.007	0.032	0.002	0.001	0.008	0.036	0.001
Ti	0.035	0.001	0.109	0.106	0.060	0.003	0.116
Fe(ii)	0.120	0.051	0.221	0.222	0.175	0.000	0.221
Mn	0.003	0.001	0.004	0.005	0.003	0.004	0.004
Mg	0.815	0.987	0.659	0.709	0.788	0.966	0.627
Ca	0.765	0.815	0.870	0.920	0.891	0.825	0.897
Na	0.067	0.033	0.038	0.035	0.036	0.048	0.043
Total	4.014	4.012	3.893	3.947	3.983	4.027	3.928
Wo	42	42	49	49	47	43	50
En	45	51	37	37	42	50	35
Fs	9	5	13	12	9	4	13
Ac	4	2	2	2	2	3	2

There are different composition cores for cpx. Rim and matrix cpx have similar composition range.

High Ti content for rim and matrix cpx is from the MgSi2 = Ti Al2 substitution. Rim and matrix cpx have higher Fe than cores.

Table . Representative mineral compositions (continued)

	Clinopyroxene			
	2EO	w25		
	cpx-mtx	lowSi	highSi-core	rim
SiO_2	44.77	48.59	51.10	47.03
TiO_2	4.09	1.58	1.16	2.79
Al_2O_3	7.74	9.15	6.29	6.72
Cr_2O_3	0.06	0.00	1.16	0.21
FeO	7.01	6.07	4.58	6.12
MnO	0.16	0.11	0.03	0.00
MgO	12.24	14.57	15.58	13.49
CaO	22.84	18.99	18.64	23.30
Na_2O	0.51	1.18	1.53	0.52
Total	99.42	100.24	100.07	100.17
	Numbers of ions on the basis of 6 O			
Si	1.636	1.775	1.867	1.718
Al(IV)	0.333	0.225	0.133	0.282
Al(VI)	0.000	0.169	0.138	0.008
Fe(iii)	0.000	0.066	0.093	0.000
Cr	0.002	0.000	0.033	0.006
Ti	0.112	0.043	0.032	0.077
Fe(ii)	0.220	0.119	0.046	0.189
Mn	0.005	0.003	0.001	0.000
Mg	0.667	0.794	0.849	0.735
Ca	0.894	0.744	0.730	0.912
Na	0.036	0.083	0.108	0.037
Total	3.905	4.021	4.030	3.963
Wo	49	41	40	49
En	37	44	46	39
Fs	12	10	8	10
Ac	2	5	6	2

Cpx in w25 was replaced by SiO2. Cpx relicts are distributed as islands in SiO2.
A few remains of rim cpx next to the edge of core cpx are preserved in w25.

Table . Representative mineral compositions (continued)

	Mg-Al chromite			
	w26		2EO	w25
SiO_2	0.00	0.07	0.00	0.08
TiO_2	0.11	0.25	0.21	0.14
Al_2O_3	32.74	36.46	30.13	31.04
Cr_2O_3	34.84	30.23	36.88	36.46
FeO	14.12	15.14	14.64	14.55
MnO	0.23	0.00	0.25	0.00
MgO	16.68	17.95	17.17	16.43
Total	98.71	100.08	99.27	98.70
Cr/Cr+Al	0.42	0.36	0.45	0.44
	Numbers of ions on the basis of 32 O			
Si	0.000	0.015	0.000	0.019
Ti	0.020	0.043	0.037	0.024
Al	8.984	9.679	8.286	8.586
Cr	6.413	5.384	6.803	6.766
Fe(iii)	0.563	0.821	0.838	0.561
Fe(ii)	2.185	2.031	2.017	2.296
Mn	0.045	0.000	0.049	0.000
Mg	5.790	6.027	5.971	5.748
Total	24	24	24	24
Spinel	$0.56MgAl_2O_4$	$0.61MgAl_2O_4$	$0.52MgAl_2O_4$	$0.54MgAl_2O_4$
Magnesiochromite	$0.16MgCr_2O_4$	$0.15MgCr_2O_4$	$0.23MgCr_2O_4$	$0.24MgCr_2O_4$
Chromite	$0.24FeCr_2O_4$	$0.19FeCr_2O_4$	$0.20FeCr_2O_4$	$0.18FeCr_2O_4$
Magnetite	$0.04FeFe_2O_4$	$0.05FeFe_2O_4$	$0.05FeFe_2O_4$	$0.04FeFe_2O_4$

Ma-Al chromites are anhedral phenocrysts with corroded rim. There are two composition groups.

Table . Representative mineral compositions (continued)

	Jacobsitic magnetite		Hematite
	w26		w25
SiO_2	0.83	SiO_2	0.21
TiO_2	17.24	TiO_2	0.74
Al_2O_3	1.57	Al_2O_3	0.85
Cr_2O_3	0.29	Cr_2O_3	0.19
FeO	63.61	Fe_2O_3	99.35
MnO	12.45	MnO	0.42
MgO	0.46	MgO	0.38
Total	96.44	Total	102.13

	Numbers of ions on the basis of 32 O
Si	0.248
Ti	3.872
Al	0.551
Cr	0.067
Fe(iii)	7.140
Fe(ii)	8.743
Mn	3.148
Mg	0.203
Total	24
Ulvospinel	$0.48Fe_2TiO_4$
Magnetite	$0.13FeFe_2^{(3+)}O_4$
Jacobsite	$0.32MnFe_2^{(3+)}O_4$

Subhedral high Mn magnetites co-exist with biotite.

Hematites distribute along the fractures in the vermiculite veins; other cations in analysis could be from impurity captured with crystals.

Table . Representative mineral compositions (continued)

	Kaersutite		Biotite		
	2EO		w26	w26-matrix	2EO
SiO_2	40.20	SiO_2	35.19	34.04	36.35
TiO_2	4.96	TiO_2	7.29	7.99	7.42
Al_2O_3	15.16	Al_2O_3	15.42	14.73	16.38
FeO	8.27	FeO	13.08	16.37	8.72
MnO	0.01	MnO	0.57	0.36	0.05
MgO	13.89	MgO	16.12	12.26	17.11
CaO	11.11	CaO	0.00	0.06	0.05
Na_2O	2.00	Na_2O	0.84	0.83	0.52
K_2O	2.52	K_2O	8.23	7.77	9.72
Total	98.13	F	0.50	0.64	0.27
		Total	97.22	95.05	96.58
	Numbers of ions on the basis of 23 O	Numbers of ions on the basis of 22 O			
Si	5.844	Si	5.185	5.229	5.262
Al(IV)	2.156	Al(IV)	2.677	2.667	2.738
Al(VI)	0.441	Al(VI)	0.000	0.000	0.056
Ti	0.542	Ti	0.808	0.923	0.807
Fe(iii)	0.139	Fe	1.611	2.103	1.055
Fe(ii)	0.866	Mn	0.071	0.047	0.006
Mn	0.001	Mg	3.540	2.808	3.692
Mg	3.010				
		Ca	0.000	0.010	0.008
Ca	1.730	Na	0.239	0.247	0.147
Na	0.564	K	1.546	1.522	1.794
K	0.467	F	0.233	0.311	0.123
Total	15.762	Total	15.678	15.555	15.566

Amphiboles exist as large subhedral phenocrysts in 2EO.
Biotites in w26 exist as intergrwoth with jacobsitic magnetite and as microphenocrysts. Biotite in 2EO is the overgrowth coating the quartz.
The micro-biotites in matrix are more Fe rich. The lower total may result from alteration (loss K).
Biotites also exist as phenocrysts, the distribution of large biotite is sparse in the rock. Our thin sections did not capture them.

Table . Representative mineral compositions (continued)

	Titanite				Apatite	
	w26	2EO	w25		w26	w25
SiO_2	30.16	30.67	30.24	SiO_2	1.15	2.06
TiO_2	32.84	31.22	33.65	TiO_2	0.12	0.11
Al_2O_3	2.64	3.57	1.29	Al_2O_3	0.12	0.37
FeO	3.46	2.66	3.21	FeO	0.82	0.92
MnO	0.12	0.07	0.00	MnO	0.05	0.07
MgO	0.12	0.00	0.00	MgO	0.13	0.46
CaO	27.37	27.49	28.81	CaO	55.19	55.11
Na_2O	0.04	0.03	0.03	Na_2O	0.13	0.07
K_2O	0.01	0.01	0.03	K_2O	0.08	0.04
P_2O_5	0.64	0.51	0.04	P_2O_5	36.49	35.49
F	0.00	0.50	0.04	F	2.11	4.04
Cl	0.10	0.04	0.01	Cl	1.45	1.79
Total	97.50	96.76	97.34	Total	97.83	100.52
	Numbers of ions on the basis of 4Si			Numbers of ions on the basis of 26 (O, F, Cl)		
Si	4	4	4	P	5.914	5.141
Ti	3.276	3.062	3.347	Ca	9.239	10.102
Al	0.412	0.548	0.201	Na	0.014	0.022
Fe(iii)	0.282	0.120	0.319	Fe	0.117	0.132
Fe(ii)	0.061	0.141		Mn	0.015	0.010
Mg	0.024	0.000	0.000	Mg	0.198	0.117
Mn	0.013	0.008	0.000	Si	0.02	0.352
Ca	3.889	3.841	4.082	Cl	0.424	1.172
Na	0.011	0.009	0.007	F	0.983	0.969
K	0.002	0.002	0.006	Total	16.923	18.017
Cl	0.025	0.010	0.003			
F	0.000	0.239	0.019			

Titanites exist as small euhedral phenocrysts and anhedral microphenocrysts in matrix.

Apatites exist as subhedral to euhedral microphenocrysts in matrix. Crystals are in needle shape about 10 to 25 um long and <2 um wide. Because the crystal size is small, there is interference from surrounding matrix in the analyses.

Table . Representative mineral compositions (continued)

	Vermiculite		
	w26	2EO	w25
SiO_2	36.66	37.11	33.37
TiO_2	0.00	0.03	0.01
Al_2O_3	12.96	13.32	15.51
Cr_2O_3	0.08	0.11	0.10
Fe_2O_3	11.92	12.15	11.23
MnO	1.40	0.94	1.63
MgO	25.28	25.58	25.56
CaO	0.67	0.24	0.22
Na_2O	0.07	0.24	0.05
K_2O	0.01	0.01	0.02
F	0.06	0.00	0.06
Cl	0.17	0.02	0.03
Total	89.27	89.76	87.77
MgO/(FeO+MgO)	0.680	0.678	0.695
	Numbers of ions on the basis of 22 O		
Si	5.388	5.404	4.999
Al	2.245	2.285	2.738
Ti	0.000	0.003	0.001
Cr	0.010	0.012	0.012
Fe(iii)	1.319	1.331	1.266
Mn	0.174	0.116	0.206
Mg	4.528	4.528	4.528
Mg	1.032	1.000	1.181
Ca	0.105	0.038	0.036
Na	0.021	0.067	0.014
K	0.002	0.002	0.003
F	0.026	0.000	0.026
Cl	0.043	0.006	0.008
Total	14.870	14.817	15.018

These vermiculites are rich in Mg and Si.

Table . Representative mineral compositions (continued)

	Orthoclase		McGillite		Pyrite			Anhydrite		Calcite
	w26		2EO		w26	2EO		w26		w26
SiO_2	69.04	SiO_2	35.18	S	54.19	54.49	FeO	0.06	FeO	0.14
Al_2O_3	20.42	Al_2O_3	0.21	Fe	44.16	47.37	MnO	0.10	MnO	0.47
FeO	0.10	FeO	10.69	Ni	0.27	0.30	MgO	0.00	MgO	0.00
MgO	0.02	MnO	42.57	Mn	0.09	0.10	CaO	42.04	CaO	55.00
CaO	0.03	MgO	0.70	Total	98.71	102.26	Na_2O	0.02	Na_2O	0.00
Na_2O	0.21	CaO	0.10				P_2O_5	0.61	P_2O_5	0.68
K_2O	10.13	Cl	3.30				F	0.03	Total	56.29
Total	99.95	Total	92.74				Cl	0.00		
							SO_3	56.93		
							Total	99.79		
			Numbers of ions on the basis of 20 O		Numbers of ions on the basis of 2 S			Numbers of ions on the basis of 4 O		
An	0.25	Si	5.872	S	2	2	Ca	1.009		
Ab	3.03	Al	0.041	Fe	0.936	0.998	S	0.997		
Or	96.72	Fe	1.492	Ni	0.005	0.006				
		Mn	6.017	Mn	0.002	0.002				
		Mg	0.173							
		Ca	0.017							
		Cl	0.933							
		Total	13.640							

Calcite analysis without CO_2.